iScience

CellPress
OPEN ACCESS

Article

Expanding the Structural Diversity of Drimentines by Exploring the Promiscuity of Two *N*-methyltransferases

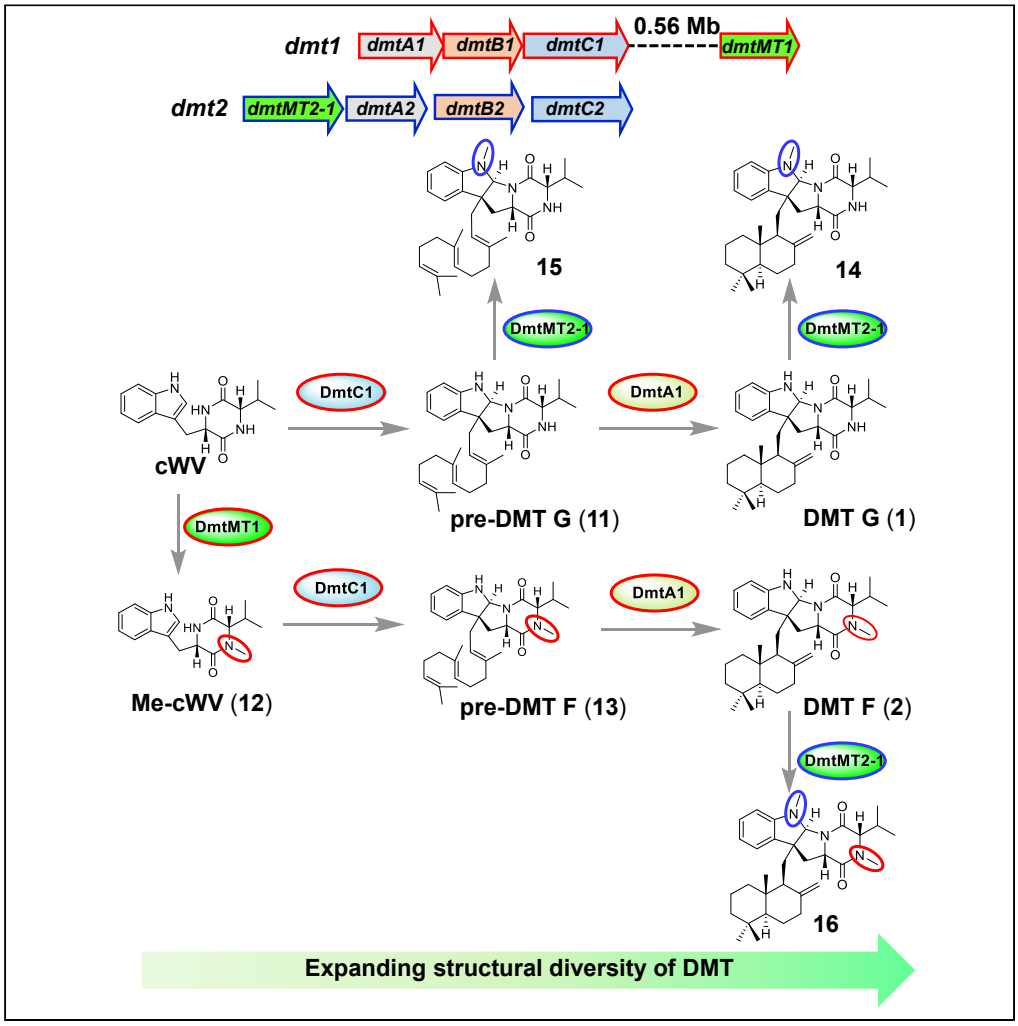

Tingting Yao, Jing Liu, Enjing Jin, ..., Tianjiao Zhu, Dehai Li, Wenli Li

liwenli@ouc.edu.cn

HIGHLIGHTS

The methylation steps during drimentines biosynthesis were unraveled

Two *N*-MTs with different regioselectivities were identified

The substrate promiscuities of DmtMT1 and DmtMT2-1 were probed

Combinatorial biosynthesis expanded the chemical space of drimentines

Yao et al., iScience *23*, 101323
July 24, 2020
https://doi.org/10.1016/j.isci.2020.101323

iScience

CellPress
OPEN ACCESS

Article

Expanding the Structural Diversity of Drimentines by Exploring the Promiscuity of Two *N*-methyltransferases

Tingting Yao,[1] Jing Liu,[1] Enjing Jin,[1] Zengzhi Liu,[1] Huayue Li,[1,2] Qian Che,[1,2] Tianjiao Zhu,[1,2] Dehai Li,[1,2] and Wenli Li[1,2,3,*]

SUMMARY

Methylation is envisioned as a promising way to rationally improve key pharmacokinetic characteristics of lead compounds. Although diverse tailoring enzymes are found to be clustered with cyclodipeptide synthases (CDPSs) to perform further modification reactions on the diketopiperazine (DKP) rings generating complex DKP-containing compounds, so far, a limited number of methyltransferases (MTs) co-occurring with CDPS have been experimentally characterized. Herein, we deciphered the methylation steps during drimentines (DMTs) biosynthesis with identification and characterization of DmtMT2-1 (from *Streptomyces* sp. NRRL F-5123) and DmtMT1 (from *Streptomyces youssoufiensis* OUC6819). DmtMT2-1 catalyzes *N*4-methylation of both pre-DMTs and DMTs; conversely, DmtMT1 recognizes the DKP rings, functioning before the assembly of the terpene moiety. Notably, both MTs display broad substrate promiscuity. Their combinatorial expression with the *dmt1* genes in different *Streptomyces* strains successfully generated eight unnatural DMT analogs. Our results enriched the MT tool-box, setting the stage for exploring the structural diversity of DKP derivatives for drug development.

INTRODUCTION

Natural products with 2,5-diketopiperazine (DKP) scaffolds are a large class of specialized metabolites with structural diversity and notable bioactivities (Borthwick, 2012). The DKP rings confer structural stability and rigidity against proteolysis, making them attractive in pharmaceutical development (Borthwick, 2012). From the biosynthetic point of view, the DKP ring is assembled *via* a traditional non-ribosomal peptide synthetase (NRPS) or a recently characterized cyclodipeptide synthase (CDPS) machinery (Belin et al., 2012). Notably, diverse tailoring enzymes are often found to be clustered with CDPSs to perform further modification reactions on the DKP rings such as oxidation (Cryle et al., 2010; Meng et al., 2018; Patteson et al., 2018), methylation (Giessen et al., 2013a, 2013b; Li et al., 2019; Liu et al., 2019; Shi et al., 2019), prenylation (Yao et al., 2018), as well as cyclization (Yao et al., 2018), generating complex DKP-containing compounds. Although relatively few tailoring enzymes co-occurring with CDPS clusters have been experimentally characterized, most of them exhibit broad substrate scopes (Giessen et al., 2013a, 2013b; Li et al., 2019; Liu et al., 2019; Tian et al., 2018; Yao et al., 2018). The small sizes and substrate promiscuities of the CDPSs and their associated tailoring enzymes highlight the CDPS pathway enzymes as potential powerful tools for the generation of structurally unique DKP compounds by combinatorial biosynthetic approaches. The use of CDPSs as "biosynthetic hooks" is thus considered an effective strategy for identifying genes modifying 2,5-DKP rings to expand the chemical space of DKPs (Borgman et al., 2019; Canu et al., 2020).

Methylation of *O*-, *C*-, *N*-, and *S*-centered nucleophiles are ubiquitous tailoring reactions during the biosynthesis of small molecules, which increases the lipophilicity and membrane permeability of small-molecule scaffolds, enhancing their membrane transport, oral bioavailability, absorption, and excretion (Barreiro et al., 2011; Liscombe et al., 2012). *N*-methylation is envisioned as a promising way to rationally improve key pharmacokinetic characteristics of cyclic peptides (Chatterjee et al., 2008). Although bioinformatics analyses indicate the presence of a large number of methyltransferases (MTs) genetically associated with CDPSs (Skinnider et al., 2018), most of them remain unexplored. Up to now, only five MTs

[1]Key Laboratory of Marine Drugs, Ministry of Education of China, School of Medicine and Pharmacy, Ocean University of China, Qingdao 266003, China

[2]Laboratory for Marine Drugs and Bioproducts of Qingdao National Laboratory for Marine Science and Technology, Qingdao, China

[3]Lead Contact

*Correspondence: liwenli@ouc.edu.cn

https://doi.org/10.1016/j.isci.2020.101323

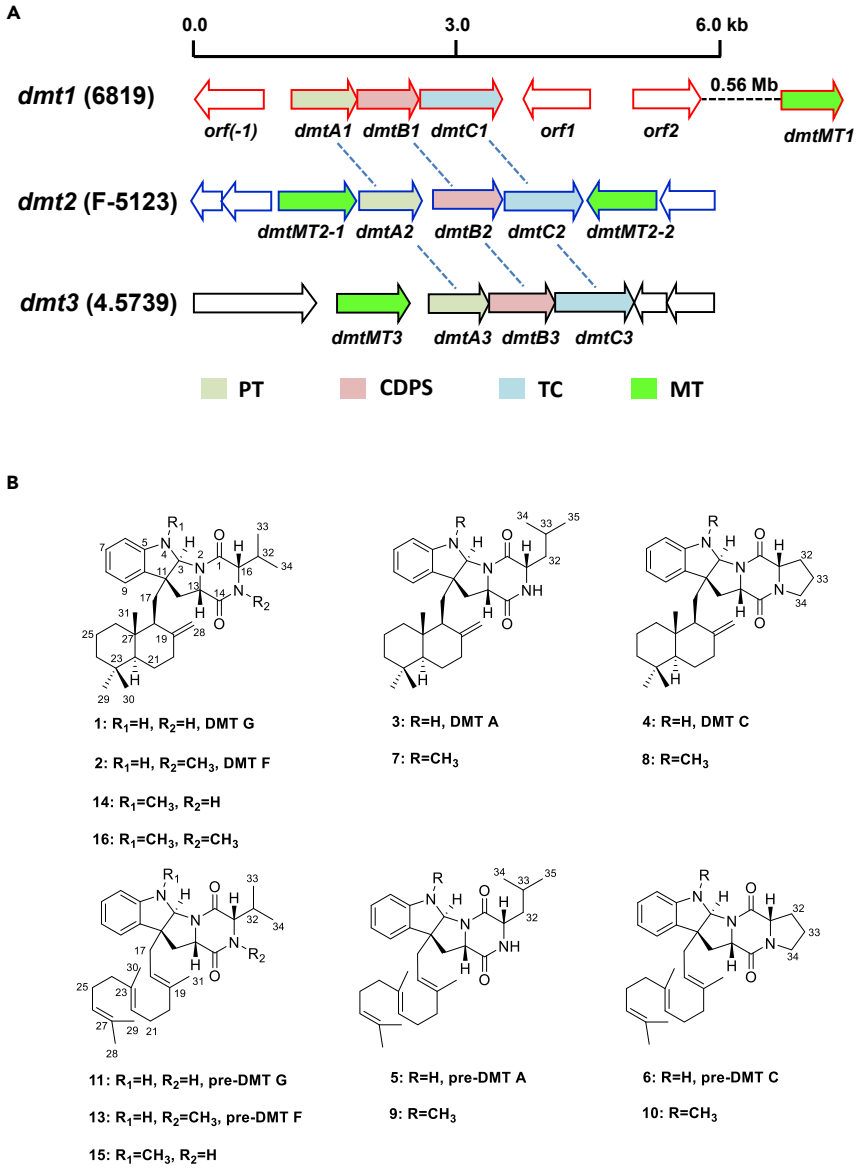

Figure 1. Genetic Organization of the *dmt1-3 loci* and Structures of Their Encoding Compounds

(A) *dmt1-3 loci* from *S. youssoufiensis* OUC6819, *Streptomyces* sp. NRRL F-5123, and *S. aidingensis* CGMCC 4.5739. PT, prenyltransferase; CDPS, cyclodipeptide synthase; TC, terpene cyclase; MT, methyltransferase.

(B) Chemical structures of drimentines, pre-drimentines, and their methylated derivatives. Compounds **7**–**10** and **13**–**16** are generated in this study.

from CDPS-dependent pathways have been functionally characterized: *O*-methyltransferase Ndas_1149 from the nocazine pathway methylating phenolic hydroxyl groups of *cyclo* (L-Phe-L-Tyr) (cFY) (Δ^3), cFY(Δ^3, Δ^6) and *cyclo* (L-Tyr-L-Tyr) (cYY) (Δ^3, Δ^6) (Giessen et al., 2013a), *N*-methyltransferase Amir_4628 catalyzing two successive *N*-methylations at the cWW ring to generate Me_2-cWW (Giessen et al., 2013b), GutE/PcmE from guanitrypmycin pathway transferring a methyl group onto the guaninyl residue (Liu et al., 2019; Shi et al., 2019), and *C*-methyltransferase StspM1 mediating *C*3-methylation of indole ring and cyclization between the indole *C2* of the Trp residue and the α-nitrogen (Li et al., 2019). These facts drive us to explore novel MTs from CDPS-dependent pathways for the generation of diverse DKP derivatives. We previously identified three homologous CDPS *loci dmt1-3* encoding drimentines (DMTs) (Figure 1, Yao et al., 2018), which are a family of terpenylated diketopiperazine alkaloids with antibacterial, antifungal, and anthelmintic activities (Che et al., 2012; Lacey et al., 1998). The CDPS DmtBs synthesize

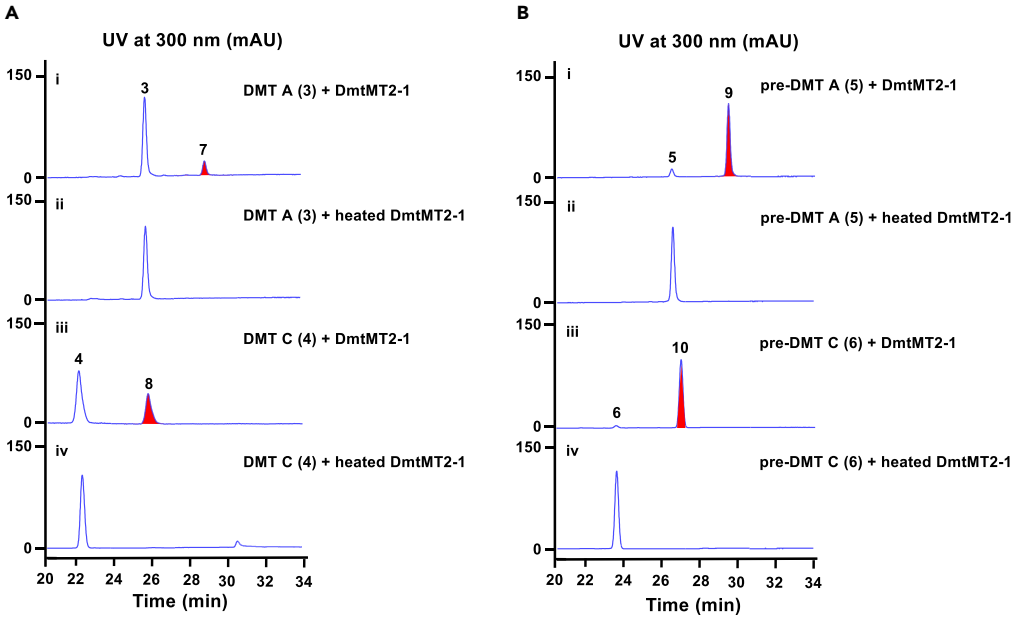

Figure 2. *In Vitro* Methyltransferase Activity of DmtMT2-1

In the presence of SAM, DmtMT2-1 converted DMT A (**3**)/C (**4**) (A) and pre-DMT A (**5**)/C (**6**) (B) to *N*4-methyl-DMT A (**7**)/C (**8**) and *N*4-methyl-pre-DMTA (**9**)/C (**10**), respectively. The red-tinted peaks represent the methylated products.
See also Figure S2 and Data S1.

cyclo (L-Trp-L-Xaa) (cWX) (X = Val, Pro, Leu, Ile or Ala), followed by prenylation and cyclization, which are, respectively, accomplished by the phytoene-synthase-like (PSL) prenyltransferase DmtCs and the membrane terpene cyclase DmtAs to afford DMTs (Yao et al., 2018). Noticeably, three putative MT genes are located adjacent to the *dmt2 locus* (from *Streptomyces* sp. NRRL F-5123) and the *dmt3 locus* (from *S. aidingensis* CGMCC 4.5739), suggesting that these two clusters might encode more complicated methylated DMTs. In contrast, no putative MT gene is found around the *dmt1 locus* from *S. youssoufiensis* OUC6819, although this strain is able to produce drimentine F (DMT F), which harbors *N*15-methyl group (Che et al., 2012). Herein, on one hand, we characterized the function of the *dmt2*- and *dmt3*-associated MT genes; on the other hand, we deciphered the *N*15-methylation step during the biosynthesis of DMT F; thereby, two *S*-adenosylmethionine (SAM)-dependent *N*-MTs (DmtMT2-1 and DmtMT1) with different regioselectivities were obtained. Their substrate spectra were probed, revealing that both of them exhibited considerable substrate promiscuities. Mixing and matching *dmtMT2-1* and *dmtMT1* with other DMT biosynthetic genes afforded unnatural methylated DMTs, providing novel effective CDPS-associated MTs for compound structural diversification.

RESULTS

Function of the MT Genes Adjacent to the *dmt Loci*

As indicated in Figure 1 and Table S3, DmtMT2-1 shows 36.7% identity/49.8% similarity to MitM (AAD28459.1), which functions as an aziridine *N*-methyltransferase during the biosynthesis of mitomycin (Varoglu et al., 2001); DmtMT2-2 shows 16.4% identity/25.3% similarity to UbiE (YP_026269.1), which catalyzes the carbon methylation reaction in the biosynthesis of ubiquinone and menaquinone (Lee et al., 1997); DmtMT3 shows 24.2% identity/34.6% similarity to PrmC (AY600244.1) of *Chlamydia trachomatis* involving in methylation of the class 1 peptide chain release factors (Pannekoek et al., 2005).

To investigate the function of these MT genes during the biosynthesis of DMTs, we solubly expressed them in *E. coli* (Figure S1) and tested their enzymatic activities *in vitro*. Given methylation may occur at different phases during DMTs biosynthesis, different substrates were subjected to assays based on the encoding products of *dmt2/3* (Yao et al., 2018). HPLC analysis of the reactions showed: (1) DmtMT2-1 was able to recognize both DMT A (**3**)/C (**4**) (Figure 2Ai and iii) and pre-DMT A (**5**)/C (**6**) (Figure 2Bi and iii), generating compounds **7**–**10**, but could not recognize cWL or cWP (Figure S2A), which indicated that a pyrroloindoline

ring is necessary for the activity of DmtMT2-1; (2) neither DmtMT2-2 (Figures S2B–S2D) nor DmtMT3 (Figures S2E and S2F) recognized the tested substrates.

Subsequently, large volume (30 mL) of reactions followed by chemical isolation was performed, leading to identification of compounds **7**–**10**. High-resolution electrospray ionization mass spectrometry (HR-ESI-MS) analysis indicated the molecular formula of **7** as $C_{33}H_{47}N_3O_2$ (*m/z* $[M + H]^+$ 518.3778, calcd 518.3747, Data S1), **8** as $C_{32}H_{43}N_3O_2$ (*m/z* $[M + H]^+$ 502.3434, calcd 502.3434, Data S1), **9** as $C_{33}H_{47}N_3O_2$ (*m/z* $[M + H]^+$ 518.3776, calcd 518.3747, Data S1), and **10** as $C_{32}H_{43}N_3O_2$ (*m/z* $[M + H]^+$ 502.3476, calcd 502.3434, Data S1), which are 14 mass units bigger than that of DMT A (**3**), DMT C (**4**), pre-DMT A (**5**), and pre-DMT C (**6**), respectively (Yao et al., 2018). Comparison of the ^1H and ^{13}C NMR data between **7** and **3** (Yao et al., 2018) revealed that they share similar structure except the presence of an additional methyl group (δ_H 2.87, δ_C 33.2) in **7** (Data S1). Based on HMBC correlation observed from the methyl proton H-36 (δ_H 2.87) to C3 (δ_C 83.6) and C5 (δ_C 150.6), we determined the methyl group is attached to the nitrogen of the dihydroindole system instead of the DKP ring (Data S1). Thus, compound **7** was determined as *N*4-methyl-DMT A. Similarly, compounds **8**–**10** are similar to DMT C (**4**), pre-DMT A (**5**), and pre-DMT C (**6**), respectively, but carry an additional methyl group (δ_H 2.88, δ_C 33.5 for **8**, δ_H 2.91, δ_C 33.2 for **9**, and δ_H 2.92, δ_C 33.5 for **10**) attached to the nitrogen of dihydroindole (Data S1). Thereby, **8**–**10** were characterized as *N*4-methyl derivatives of compounds **4**–**6**. The above results supported that DmtMT2-1 is responsible for the *N*4-methylation during DMTs biosynthesis, which may happen before or after cyclization. It was worth to mention that methylation occurs only at *N*15 in all the reported methylated DMTs (DMT F, H, and I). Thus, the *N*4-methyltransferase DmtMT2-1 would expand the diversity of DMTs compounds.

Probing the MT Gene Involved in *N*15-Methylation of DMT F

Although no MT gene is found adjacent to *dmt1*, *S. youssoufiensis* OUC6819 is able to produce DMT F, which harbors a methyl group at *N*15 position. This fact indicates that the responding MT gene is located in another place of the genome. With comparative liquid chromatography-mass spectrometry (LC-MS) analysis of the fermentation products from the OUC6819 strains, a compound peak with molecular weight of 14 Daltons bigger than that of cWV (*m/z* $[M + H]^+$ calcd 286.1556; Figure S3B) was observed in *ΔdmtC1* (the prenyltransferase gene in charge of the assembly of farnesyl group onto cWV) (Figure S3Aii) and the *dmtB1* overexpression strain (Figure S3Aiii) but not in the wild-type strain (Figure S3Ai). This phenotype led us to hypothesize that methylation may happen before the assembly of the terpene moiety. Therefore, Amir_4628, which conducts two successive *N*-methylations at the DKP ring (Giessen et al., 2013b), was subjected to BLAST against the OUC6819 genome, revealing a homologous gene *6880MT* (renamed as *dmtMT1*; 33.5% identity/45.0% similarity to Amir_4628) at 0.56 Mb upstream of the *dmt1 locus* (Figure 1, Table S3).

To detect if *dmtMT1* is involved in the biosynthesis of DMT F, in-frame deletion was performed, generating *ΔdmtMT1* (Figure S4). HPLC analysis revealed that the production of DMT F was completely abolished; conversely, DMT G was still produced in *ΔdmtMT1* albeit in small amount (Figure 3ii). Moreover, complementation of *ΔdmtMT1* restored the production of DMT F (Figure 3iii); overexpression of *dmtMT1* resulted in increased production of DMT F by about 2-fold (Figure 3iv). These results ambiguously demonstrated *dmtMT1* to be responsible for the *N*15-methylation of DMT F.

Timing of the *N*15-Methylation during DMT F Biosynthesis

To identify the exact timing of the methylation step, *in vitro* biochemical reactions were carried out using cWV, pre-DMT G (**11**), and DMT G (**1**) as substrates. As indicated in Figure 4, DmtMT1 was capable of recognizing cWV to give a new peak (Figure 4A) but could not accept pre-DMT G or DMT G (Figure S5), supporting the methyl group is assembled right after the formation of cWV. Time course analysis showed that only a single methylation takes place, as indicated by the presence of the sole product with a molecular ion peak $[M + H]^+$ at *m/z* 300.1726, which was 14 units bigger than that of cWV (*m/z* $[M + H]^+$ calcd 286.1556) (Figures 4A and 4B).

To clarify the position of the methylation, HR-ESI-MS^2 analysis was conducted. As shown in Figure 4B, in addition to the characteristic fragmentation pattern of 2,5-DKP with neutral losses of 28 Da (-CO) and 45 Da (-$HCONH_2$) (Guo et al., 2009), successive neutral loss of 59 Da corresponding to a $HCONHCH_3$ fragment could also be detected, suggesting that the methylation takes place at the DKP ring; the protonated substituent ion at *m/z* 130 indicated the presence of tryptophan (Guo et al., 2009); the ions at *m/z* 169.0984, 183.1130 resulting from elimination of 3-methyl-1-H-indole and indole, respectively, combined with *m/z* 86.0964 from sequential losses of CO and Trp residue proved that the methyl group is attached to the

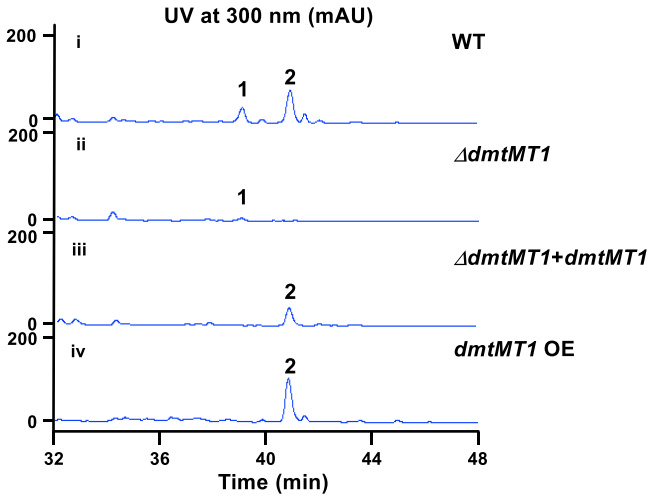

Figure 3. HPLC Analysis of the Fermentation Products from OUC6819 Strains

(i) WT, wild-type strain; (ii) *ΔdmtMT1*; (iii) *ΔdmtMT1 + dmtMT1*, genetic complementation strain of *ΔdmtMT1*; (iv) *dmtMT1* OE, overexpression strain of *dmtMT1*.

α-nitrogen of Val in cWV, which was further confirmed by the HMBC correlation of Me-cWV (**12**) from the methyl proton H-20 (δ_H 2.82) to C12 (δ_C 166.0) and C14 (δ_C 66.6) (Figure 4C and Data S1).

This fact means the PSL-family prenyltransferase DmtC1, which transfers farnesyl group onto cWV to generate pre-DMT G (Yao et al., 2018), should be able to recognize Me-cWV as well. Thus, we incubated DmtC1 with Me-cWV (**12**) in the presence of farnesyl diphosphate (FPP), and a new compound (**13**) appeared as expected (Figure S6), with a molecular ion peak $[M + H]^+$ at *m/z* 504.3579, which was 14 units bigger than that of pre-DMT G (Data S1). The ^1H and ^{13}C NMR spectra of **13** provided a dataset similar to that of pre-DMT G, with the chemical shift difference observed for a methyl group (δ_H 2.81, δ_C 32.7) (Data S1). The absence of one-proton singlet at δ_H 7.92 in pre-DMT G indicated that the methyl group was attached to *N*15 as confirmed by the strong HMBC correlation from the methyl proton H-35 (δ_H 2.81) to C14 (δ_C 165.1) and C16 (δ_C 66.3) (Data S1). Considering the biosynthetic assembly line of DMT G, we proposed that compound **13** is the biosynthetic precursor of DMT F, and thus it was named as pre-DMT F, which would be further cyclized by the terpene cyclase DmtA1 to afford DMT F.

PROBING SUBSTRATE PROMISCUITY OF DMTMT2-1 AND DMTMT1

With the two methyltransferases (DmtMT2-1 and DmtMT1) in hand, we evaluated their potentials as tool enzymes to diversify structures of DMT compounds. For DmtMT2-1, another two substrates, DMT G (**1**) and pre-DMT G (**11**), were tested. As shown in Figure 5A, both of them were recognized by DmtMT2-1, transforming **1** into **14** and **11** into **15** as expected. All the products were isolated and their structures elucidated by HR-ESI-MS and NMR analyses (Data S1). Finally, **14** (*m/z* $[M + H]^+$ 504.3630, calcd 504.3590) and **15** (*m/z* $[M + H]^+$ 504.3647, calcd 504.3590) were determined to be *N*4-methyl-DMT G and *N*4-methyl-pre-DMT G as indicated by the HMBC correlations from the methyl proton H-35 (δ_H 2.86 for **14** and δ_H 2.91 for **15**) to C3 (δ_C 83.6 for **14** and δ_C 84.2 for **15**) and C5 (δ_C 150.8 for **14** and δ_C 150.9 for **15**) (Data S1).

To probe the substrate promiscuity of DmtMT1, a series of DKPs were tested. Delightedly, DmtMT1 exhibited broad substrate flexibility and was able to recognize a bunch of DKPs, including cWL, cWI, cWA, cWT, cWF, cWY, cWW, and noticeably *cyclo* (D-Trp-L-Val) (cDWV) and cYV as well (the nomenclature of a cyclodipeptide is indicated here by the one-letter code for the two L-configured amino acids) (Figure 5B and Data S2). The responding methylated DKPs were identified by HR-ESI-MS^2 analysis (Data S2). Their fragmentation patterns were in agreement with that of Me-cWV (Figure 4B), supporting that each *N*-methylation regio-specifically occurs at the position derived from the second amino acid (from the biosynthetic point of view). Based on the relative catalytic efficiencies, we can clearly see DmtMT1 prefers cWXs with X being aliphatic over aromatic amino acids (Figure 5B). Delightedly, DmtMT1 was capable of transferring the methyl group onto cDWV and cYV, albeit at much lower efficiencies, implying it has certain flexibility toward the first amino acid as well.

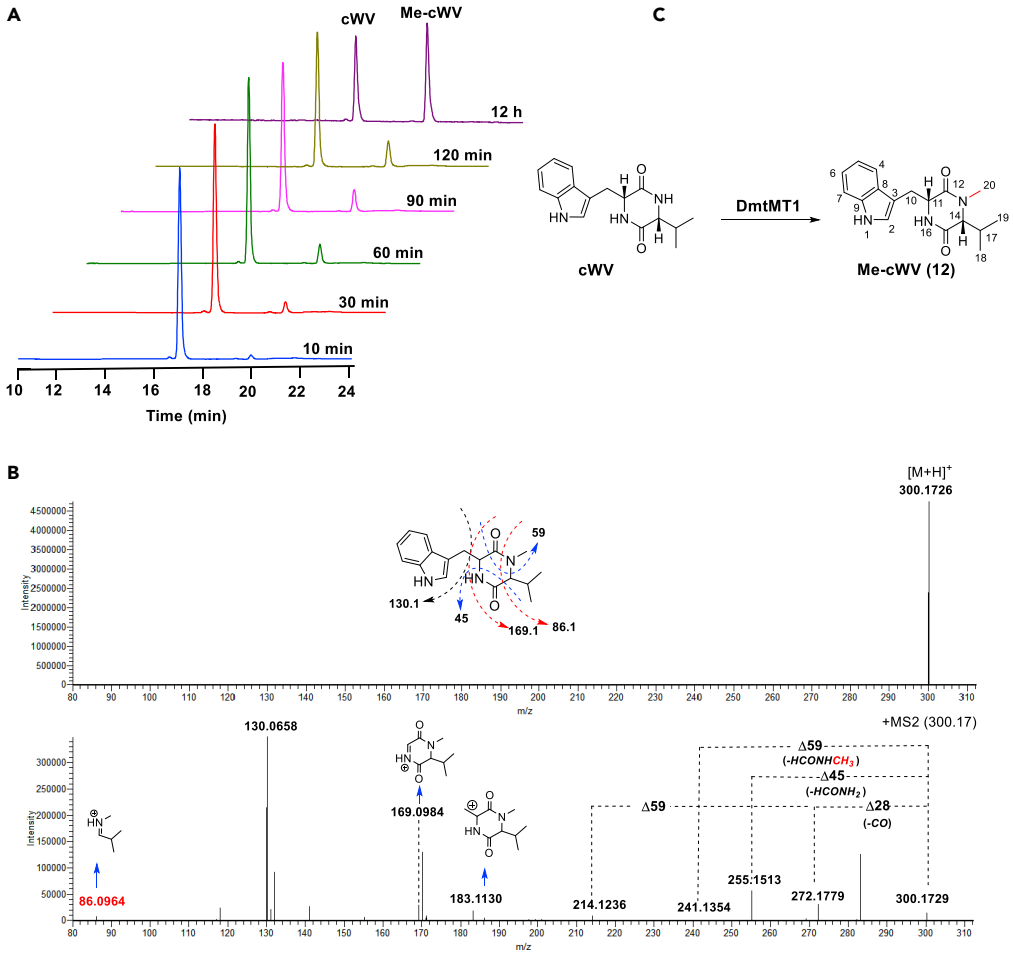

Figure 4. *In Vitro* Methyltransferase Activity of DmtMT1

(A) Time course experiment of the DmtMT1-catalyzed reaction using cWV as substrate. Chromatograms show the absorbance at 280 nm.

(B) HR-ESI-MS^2 fragmentation spectrum of Me-cWV (*m/z* 300.1726).

(C) Schematic representation of DmtMT1-catalyzed reaction illustrated by using cWV as substrate.

See also Figure S5.

The above results indicated that both DmtMT2-1 and DmtMT1 are *N*-methyltransferases with broad substrate promiscuity and stringent regiospecificity, which would potentially serve as efficient catalysts for structural diversification in drug development.

GENERATION OF UNNATURAL DMTS BY USING THE LOGIC OF SYNTHETIC BIOLOGY

The availability of these two MTs drove us to further generate unnatural DMT analogs by using the logic of synthetic biology. Based on the biosynthetic machinery of DMTs, we introduced *dmtMT2-1* or/and *dmtMT1* into different cells, including DMTs producer *S. youssoufiensis* OUC6819, *S. coelicolor* M1146/*dmtB1C1* (accumulating pre-DMTs), and *S. coelicolor* M1146/*dmtA1B1C1* (producing DMTs) (Yao et al., 2018).

As shown in Figure 6, expression of *dmtMT2-1* in *S. coelicolor* M1146/*dmtB1C1* led to the appearance of three small peaks, which were identified to be methylated pre-DMT compounds **10**, **15**, and **9**, respectively (Figure 6iii and iv). When *dmtMT2-1* was introduced into *S. youssoufiensis* OUC6819, in addition to **14**, another compound peak **16** showed up (Figure 6vi and vii). Considering the regioselectivity of *dmtMT2-1*, we speculated **16** might be *N*4-methyl-DMT F, which was confirmed by HR-ESI-MS (Data S1) and NMR data with the presence of the methyl group (δ_H 2.85, δ_C 31.4), along with its strong HMBC correlations to C3 (δ_C 82.8) and C5 (δ_C 151.5) (Data S1).

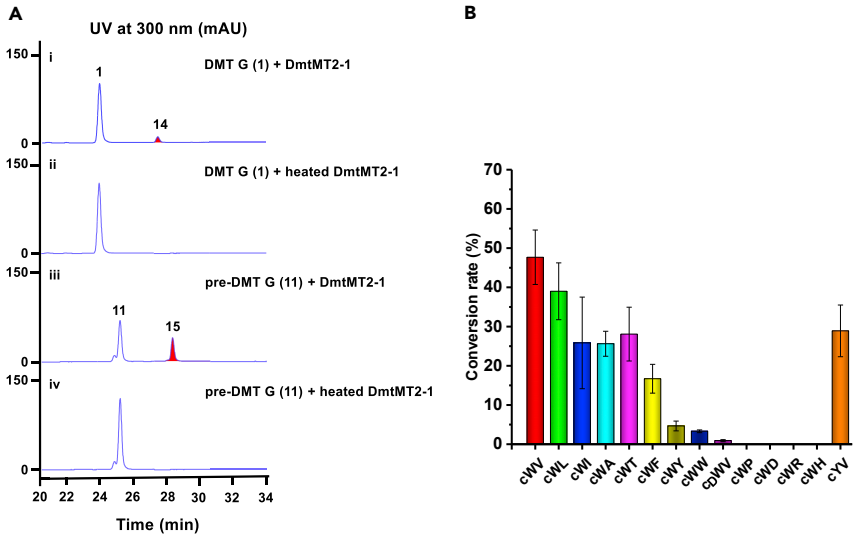

Figure 5. Substrate Promiscuities of DmtMT2-1 and DmtMT1

(A) HPLC traces of DmtMT2-1-catalyzed reactions using DMT G (**1**) and pre-DMT G (**11**) as substrates.

(B) Histogram of the conversion rates of DmtMT1 regarding different cyclodipeptides. The relative production amounts are obtained by comparison with the respective substrate calculated using UV trace integrals. Error bars represent ±SD of three independent experiments. HPLC traces and HR-ESI-MS^2 spectra of each reaction are shown in Data S2.

Expression of *dmtMT1* in *S. coelicolor* M1146/*dmtB1C1* led to decreased amount of **11** and simultaneous accumulation of pre-DMT F (**13**) (Figure 6viii and ix). When introducing *dmtMT1* into *S. coelicolor* M1146/*dmtA1B1C1*, DMT F (**2**) was accumulated as expected (Figure 6xi and xii). Unfortunately, no new product was observed after further introduction of *dmtMT2-1* into *S. coelicolor* M1146/*dmtB1C1* + *dmtMT1* (Figure 6xiii).

DISCUSSION

CDPSs are small enzymes that utilize two aminoacyl-tRNAs to catalyze the formation of a 2,5-DKP ring system (Gondry et al., 2009). To date, over 110 CDPSs have been functionally characterized and usually exhibit a certain degree of substrate promiscuity, making CDPSs intriguing members of Nature's biosynthetic repertoire (Canu et al., 2020). The resulting cyclodipeptides are generally further modified by at least one tailoring enzyme adjacent to CDPS, including formation of C-C bond and C-O bond, and regioselective methylation and prenylation (Borgman et al., 2019). In this study, we identified and characterized two promiscuous *N*-methyltransferases and elucidated the methylation machinery during DMTs biosynthesis through *in vivo* and *in vitro* experiments, providing significant insights into generation of DKP derivatives by using synthetic biology approaches.

Although both DmtMT2-1 and DmtMT1 are involved in DMT biosynthesis, they act at different timings with different manners of function. As indicated in Figure 7, in OUC6819, the methyl group is assembled right after the formation of cWV instead of happening as the last step, and the following prenylation and cyclization steps occur in parallel, indicating both DmtC1 and DmtA1 display flexible substrate promiscuity as well, which should be exploited further. Conversely, as a novel dihydroindole *N*-methyltransferase, DmtMT2-1 from *Streptomyces* sp. NRRL F-5123 functions after indole *C*3-normal prenylation, recognizing pre-DMTs, DMTs, and *N*15-methyl-DMTs. Such big structural differences between their substrates are in accordance with the low similarity/identity (29.5%/17.4%) between DmtMT2-1 and DmtMT1. Notably, mixing and matching of *dmtMT2-1* and *dmtMT1* with other DMT biosynthetic genes leads to generation of "unnatural" natural products *N*4-methyl-DMT G (**14**), *N*4-methyl-pre-DMT G (**15**), and *N*4-methyl-DMT F (**16**).

In microbes, the genes responsible for production of a specialized metabolite are mostly found in close proximity to another in dedicated biosynthetic gene clusters. However, *dmtMT1* is located at 0.56 Mb downstream of the *dmt1* locus. In comparison with its homolog Amir_4628, which doubly methylates DKPs constituting two identical aromatic amino acids (Giessen et al., 2013b), DmtMT1 prefers cWX with X being aliphatic amino acids and strictly methylates nitrogen originating from the X residue. Noticeably, DmtMT1 displays remarkable

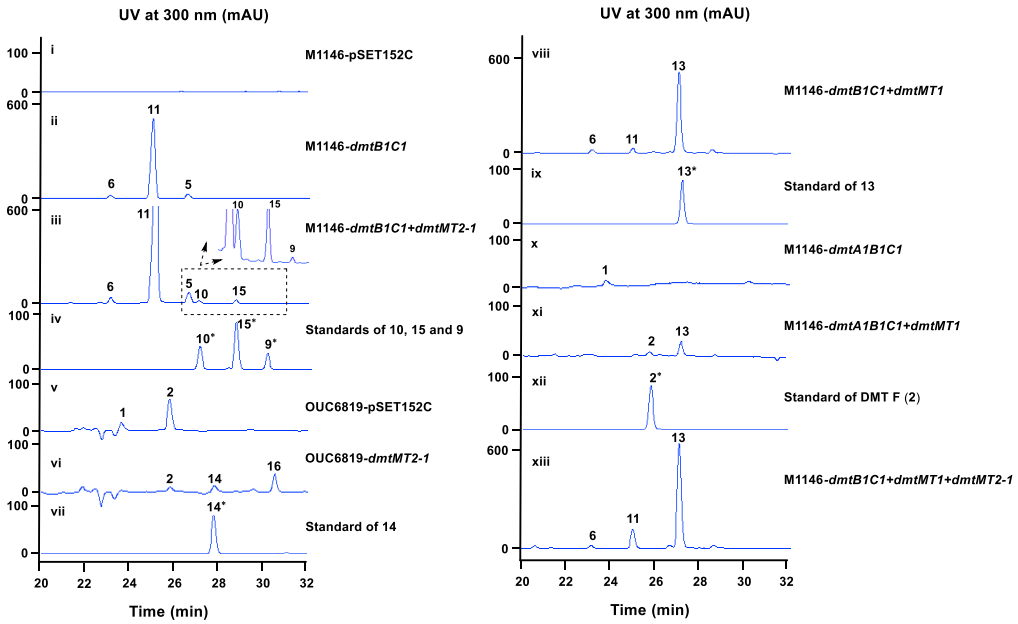

Figure 6. Combinatorial Expression of *dmtMT1* and/or *dmtMT2-1* with *dmt1* Genes

substrate promiscuity. It allows the second amino acid to be Phe and Tyr and even admits the first amino acid to be D-configured Trp and Tyr, making DmtMT1 a very promising tool enzyme for compound diversification.

With the advent of next-generation sequencing, massive microbial genome sequence data have been uploaded to the public domain. Simple BLAST-based searches reveal large numbers of MTs associated with CDPSs in prokaryotic genomes. Hence, we constructed a sequence similarity network from selected MT sequences and assigned them to known MTs. As indicated in Figure S7, three MT homologs (WP_055513754.1, WP_029387245.1, and WP_078513178.1) clustered with DmtMT2-1 are associated with a CDPS and a PSL-prenyltransferase, indicating that they might be involved in the biosynthesis of novel DMT-like compounds; noticeably, another four DmtMT2-1 homologs (StspM2/StflM2/5971M2/StalM2) are proposed to be involved in the *N*-methylation step during nocardioazine biosynthesis, but no *in vivo* nor *in vitro* results are provided (Li et al., 2019). Our results would enlighten deciphering of the methylation steps of nocardioazine-like natural products. Moreover, there are still several MTs that are not clustered with any known MTs, suggesting the untapped potentials of MTs as sources of new catalysts.

Apart from methyltransferases, we note that several other ORFs are in close proximity to CDPSs in cluster *dmt2/3*, such as the cyclodipeptide oxidases (CDOs), which have been reported to catalyze Cα-Cβ dehydrogenations on diverse cyclodipeptides (Giessen et al., 2013a; Lautru et al., 2002). Thus, further experiments are required to completely characterize the functions of these proteins and gain a broader understanding of DMTs biosynthesis.

Limitations of the Study

The molecular mechanism underlying the promiscuity of DmtMT1 and DmtMT2-1 has not been elucidated in the present study. Future crystallographic studies and systematic structure-guided mutagenesis would shed light on these issues.

Resource Availability

Lead Contact

Further information and requests for resources and reagents should be directed to and will be fulfilled by the Lead Contact, Prof. Dr. Wenli Li (email: liwenli@ouc.edu.cn).

Materials Availability

All unique/stable reagents generated in this study are available from the Lead Contact without restriction.

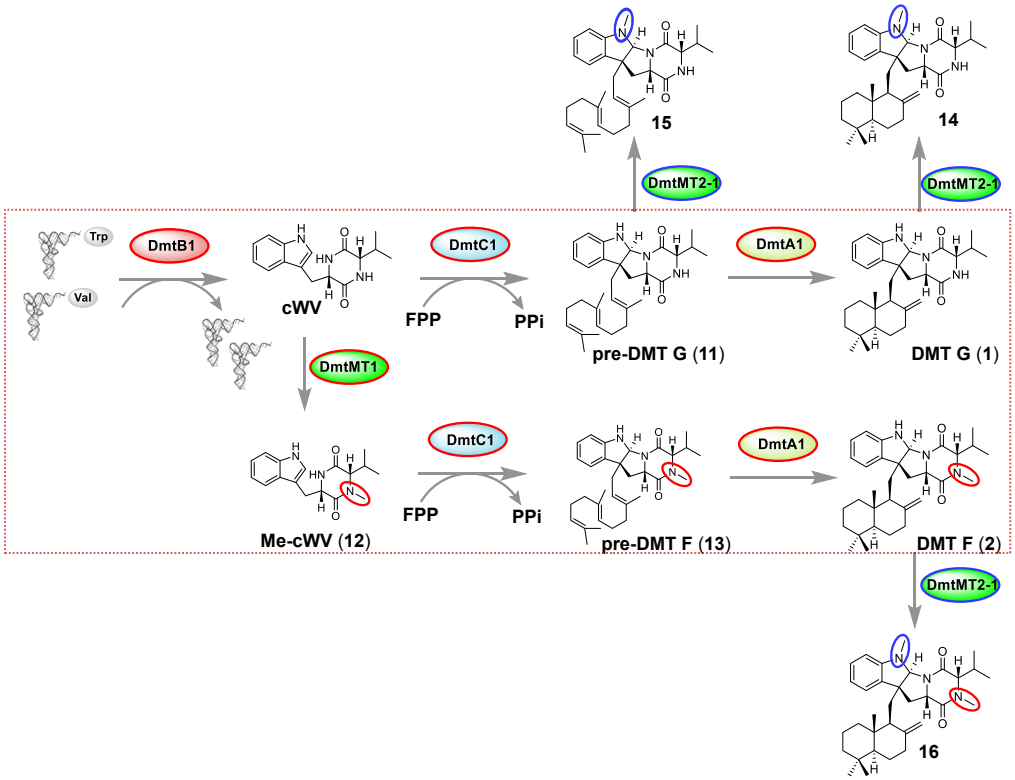

Figure 7. Assembly Lines of Drimentines Occurring in *S. youssoufiensis* OUC6819 (highlighted in red rectangle box) and *S. coelicolor* M1146/*dmtB1C1+dmtMT2-1*

Data and Code Availability

The accession number for the *dmtMT1* reported in this paper is GenBank: MK894429 (https://www.ncbi.nlm.nih.gov/nuccore/MK894429.1). All relevant data supporting the findings of this study are available within the paper and its Supplemental Information files. Additional data are provided upon reasonable request.

METHODS

All methods can be found in the accompanying Transparent Methods supplemental file.

SUPPLEMENTAL INFORMATION

Supplemental Information can be found online at https://doi.org/10.1016/j.isci.2020.101323.

ACKNOWLEDGMENTS

This work was supported by grants from the National Key R&D Program of China (2019YFC0312501), the National Natural Science Foundation of China (U1706206, 81991525, 31900049, 31570032, 31711530219 & 31171201), and the China Postdoctoral Science Foundation (2019M652483).

AUTHOR CONTRIBUTIONS

Conceptualization, W.L.; Methodology, J.L. and Z.L.; Investigation, T.Y. and E.J.; Formal Analysis, H.L.; Writing – Original Draft, W.L. and T.Y.; Writing – Review & Editing, W.L. and T.Y.; Funding Acquisition, W.L. and T.Y.; Resources, Q.C., T.Z., and D.L.; Supervision, W.L.

DECLARATION OF INTERESTS

The authors declare no competing interests.

Received: May 13, 2020
Revised: June 12, 2020
Accepted: June 25, 2020
Published: July 24, 2020

REFERENCES

Barreiro, E.J., Kümmerle, A.E., and Fraga, C.A. (2011). The methylation effect in medicinal chemistry. Chem. Rev. *111*, 5215–5246.

Belin, P., Moutiez, M., Lautru, S., Seguin, J., Pernodet, J.L., and Gondry, M. (2012). The nonribosomal synthesis of diketopiperazines in tRNA-dependent cyclodipeptide synthase pathways. Nat. Prod. Rep. *29*, 961–979.

Borgman, P., Lopez, R.D., and Lane, A.L. (2019). The expanding spectrum of diketopiperazine natural product biosynthetic pathways containing cyclodipeptide synthases. Org. Biomol. Chem. *17*, 2305–2314.

Borthwick, A.D. (2012). 2,5-Diketopiperazines: synthesis, reactions, medicinal chemistry, and bioactive natural products. Chem. Rev. *112*, 3641–3716.

Canu, N., Moutiez, M., Belin, P., and Gondry, M. (2020). Cyclodipeptide synthases: a promising biotechnological tool for the synthesis of diverse 2,5-diketopiperazines. Nat. Prod. Rep. *37*, 312–321.

Chatterjee, J., Gilon, C., Hoffman, A., and Kessler, H. (2008). *N*-methylation of peptides: a new perspective in medicinal chemistry. Acc. Chem. Res. *41*, 1331–1342.

Che, Q., Zhu, T., Qi, X., Mandi, A., Kurtan, T., Mo, X., Li, J., Gu, Q., and Li, D. (2012). Hybrid isoprenoids from a reeds rhizosphere soil derived actinomycete *Streptomyces* sp. CHQ-64. Org. Lett. *14*, 3438–3441.

Cryle, M.J., Bell, S.G., and Schlichting, I. (2010). Structural and biochemical characterization of the cytochrome P450 CypX (CYP134A1) from *Bacillus subtilis*: a *cyclo*-L-leucyl-L-leucyl dipeptide oxidase. Biochemistry *49*, 7282–7296.

Giessen, T.W., von Tesmar, A.M., and Marahiel, M.A. (2013a). Insights into the generation of structural diversity in a tRNA-dependent pathway for highly modified bioactive cyclic dipeptides. Chem. Biol. *20*, 828–838.

Giessen, T.W., von Tesmar, A.M., and Marahiel, M.A. (2013b). A tRNA-dependent two-enzyme pathway for the generation of singly and doubly methylated ditryptophan 2,5-diketopiperazines. Biochemistry *52*, 4274–4283.

Gondry, M., Sauguet, L., Belin, P., Thai, R., Amouroux, R., Tellier, C., Tuphile, K., Jacquet, M., Braud, S., Courcon, M., et al. (2009). Cyclodipeptide synthases are a family of tRNA-dependent peptide bond-forming enzymes. Nat. Chem. Biol. *5*, 414–420.

Guo, Y., Cao, S., Zong, X., Liao, X., and Zhao, Y. (2009). ESI-MS^n study on the fragmentation of protonated cyclic-dipeptides. Spectroscopy *23*, 131–139.

Lacey, E., Power, M., Wu, Z., and Rickards, R. (1998). Terpenylated Diketopiperazines,(drimentines) (Patent Int. Appl.), WO9809968 A1.

Lautru, S., Gondry, M., Genet, R., and Pernodet, J. (2002). The albonoursin gene cluster of *S. noursei*: biosynthesis of diketopiperazine metabolites independent of nonribosomal peptide synthetases. Chem. Biol. *9*, 1355–1364.

Lee, P.T., Hsu, A.Y., Ha, H.T., and Clarke, C.F. (1997). A *C*-methyltransferase involved in both ubiquinone and menaquinone biosynthesis: isolation and identification of the *Escherichia coli ubiE* gene. J. Bacteriol. *179*, 1748–1754.

Li, H., Qiu, Y., Guo, C., Han, M., Zhou, Y., Feng, Y., Luo, S., Tong, Y., Zheng, G., and Zhu, S. (2019). Pyrroloindoline cyclization in tryptophan-containing cyclodipeptides mediated by an unprecedented indole *C*3 methyltransferase from *Streptomyces* sp. Hph0547. Chem. Commun. *55*, 8390–8393.

Liscombe, D.K., Louie, G.V., and Noel, J.P. (2012). Architectures, mechanisms and molecular evolution of natural product methyltransferases. Nat. Prod. Rep. *29*, 1238–1250.

Liu, J., Xie, x., and Li, S.-M. (2019). Guanitrypmycin biosynthetic pathways imply Cytochrome P450-mediated regio-and stereospecific guaninyl transfer reactions. Angew. Chem. *58*, 11534–11540.

Meng, S., Han, W., Zhao, J., Jian, X., Pan, H., and Tang, G. (2018). A six-oxidase cascade for tandem C−H bond activation revealed by reconstitution of bicyclomycin biosynthesis. Angew. Chem. *57*, 719–723.

Pannekoek, Y., Heurgue-Hamard, V., Langerak, A.A., Speijer, D., Buckingham, R.H., and van der Ende, A. (2005). The *N*5-glutamine *S*-adenosyl-L-methionine-dependent methyltransferase PrmC/HemK in *Chlamydia trachomatis* methylates class 1 release factors. J. Bacteriol. *187*, 507–511.

Patteson, J.B., Cai, W., Johnson, R.A., Santa Maria, K.C., and Li, B. (2018). Identification of the biosynthetic pathway for the antibiotic bicyclomycin. Biochemistry *57*, 61–65.

Shi, J., Xu, X., Zhao, E.J., Zhang, B., Li, W., Zhao, Y., Jiao, R.H., Tan, R.X., and Ge, H.M. (2019). Genome mining and enzymatic total biosynthesis of purincyclamide. Org. Lett. *21*, 6825–6829.

Skinnider, M.A., Johnston, C.W., Merwin, N.J., Dejong, C.A., and Magarvey, N.A. (2018). Global analysis of prokaryotic tRNA-derived cyclodipeptide biosynthesis. BMC Genom. *19*, 45.

Tian, W., Sun, C., Zheng, M., Harmer, J.R., Yu, M., Zhang, Y., Peng, H., Zhu, D., Deng, Z., and Chen, S.-L. (2018). Efficient biosynthesis of heterodimeric C^3-aryl pyrroloindoline alkaloids. Nat. Commun. *9*, 1–9.

Varoglu, M., Mao, Y., and Sherman, D.H. (2001). Mapping the mitomycin biosynthetic pathway by functional analysis of the MitM aziridine *N*-methyltransferase. J. Am. Chem. Soc. *123*, 6712–6713.

Yao, T., Liu, J., Liu, Z., Li, T., Li, H., Che, Q., Zhu, T., Li, D., Gu, Q., and Li, W. (2018). Genome mining of cyclodipeptide synthases unravels unusual tRNA-dependent diketopiperazine-terpene biosynthetic machinery. Nat. Commun. *9*, 4091.

iScience, Volume *23*

Supplemental Information

Expanding the Structural Diversity of Drimentines by Exploring the Promiscuity of Two *N*-methyltransferases

Tingting Yao, Jing Liu, Enjing Jin, Zengzhi Liu, Huayue Li, Qian Che, Tianjiao Zhu, Dehai Li, and Wenli Li

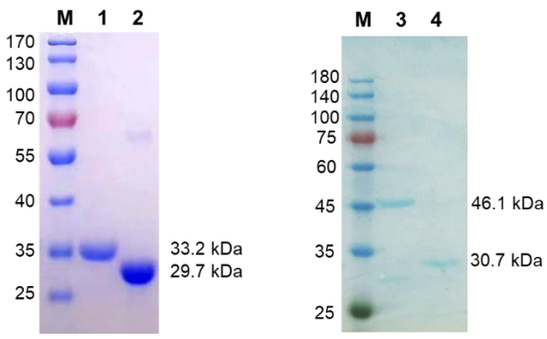

Figure S1. SDS-PAGE gels of DmtMT2-1 (lane 1), DmtMT1 (lane 2), DmtMT2-2 (lane 3) and DmtMT3 (lane 4), Related to Figures 2, and 4-5.

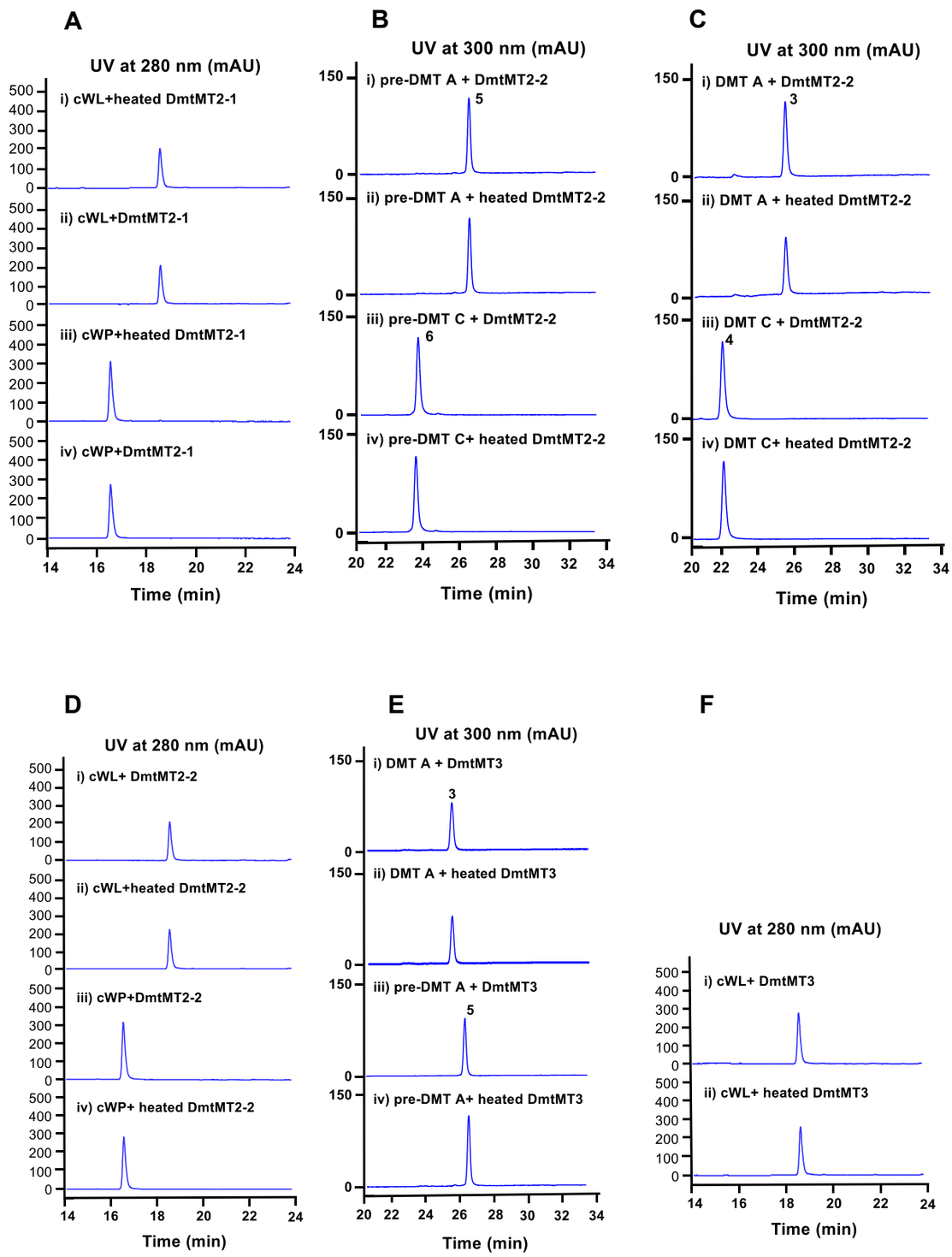

Figure S2. *In vitro* assays of DmtMT2-1, DmtMT2-2 and DmtMT3, Related to Figure 2.

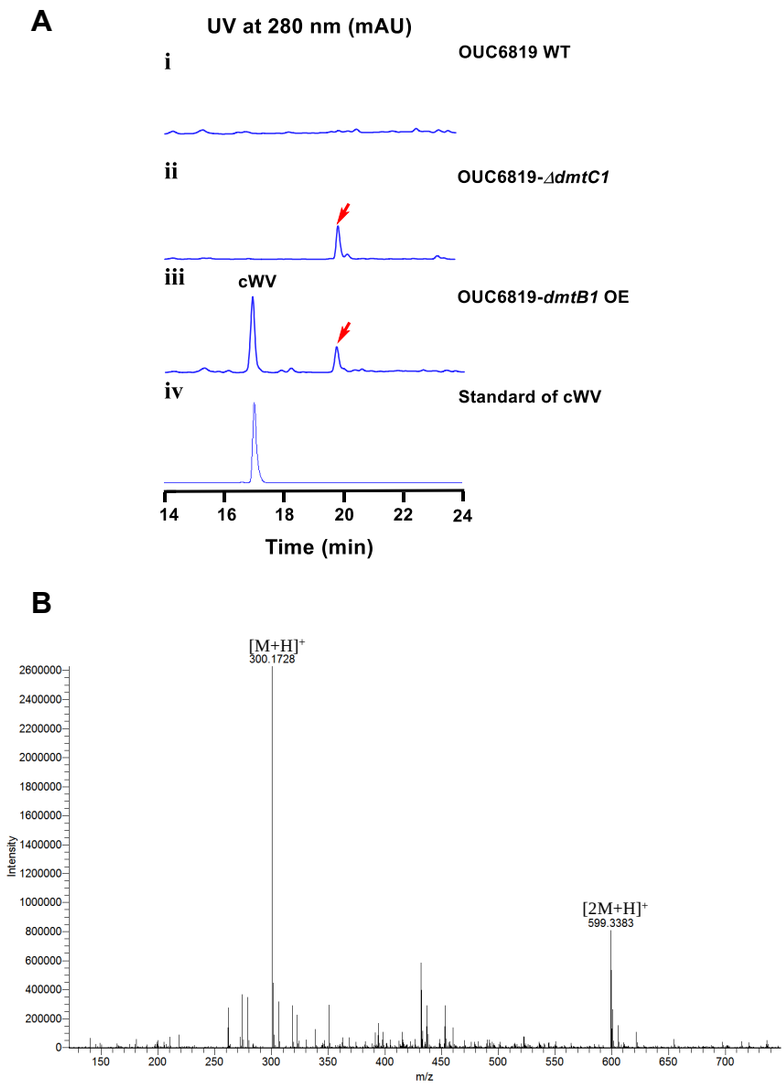

Figure S3. (A) HPLC traces of the fermentation products from (i) the wild-type OUC6819 strain; (ii) *ΔdmtC1*; (iii) overexpression of *dmtB1* in *S. youssoufiensis* OUC6819; (iv) standard of cWV. (B) The HR-ESI-MS spectrum of the compound peak indicated by red arrow, Related to Figure 3.

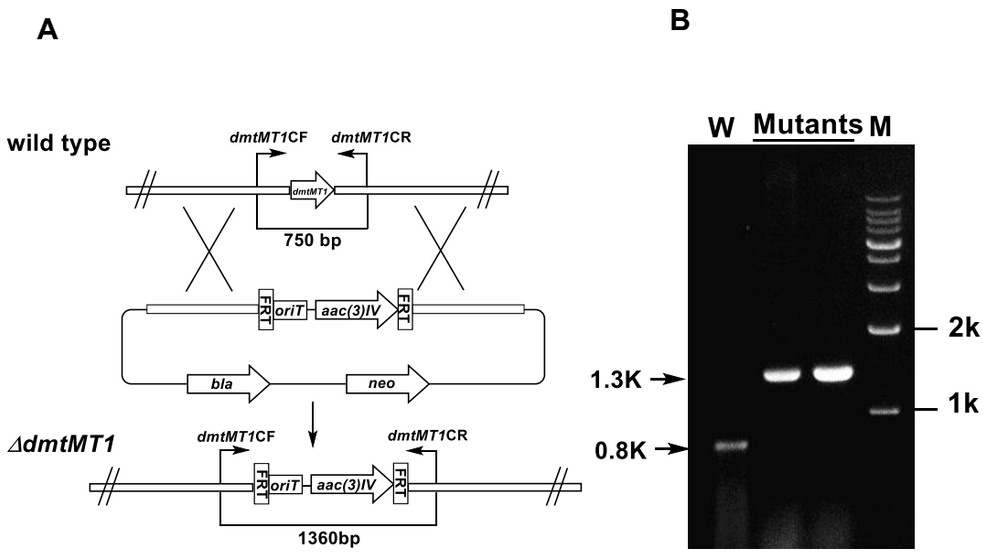

Figure S4. Inactivation of *dmtMT1*. (A) Construction of the Δ*dmtMT1* mutant. (B) PCR confirmation of the Δ*dmtMT1* mutant. M: DNA marker; W: *S. youssoufiensis* OUC6819 wild-type strain; Mutant: the Δ*dmtMT1* mutant, Related to Figure 3.

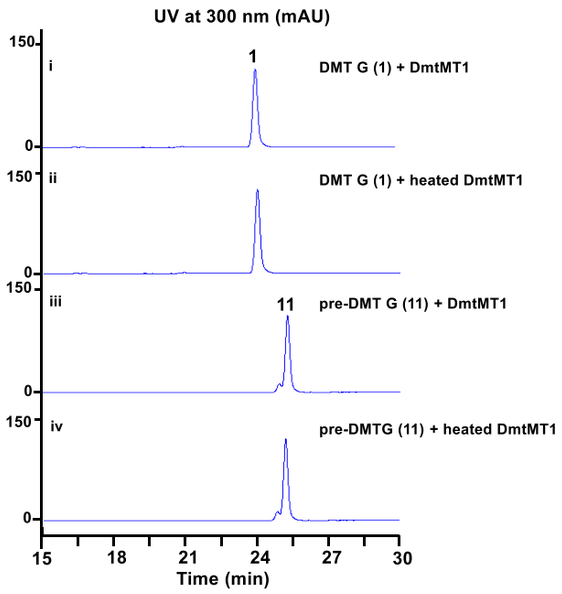

Figure S5. *In vitro* methyltransferase activity of DmtMT1 using DMT G (**1**) and pre-DMT G (**11**) as substrates, Related to Figure 4.

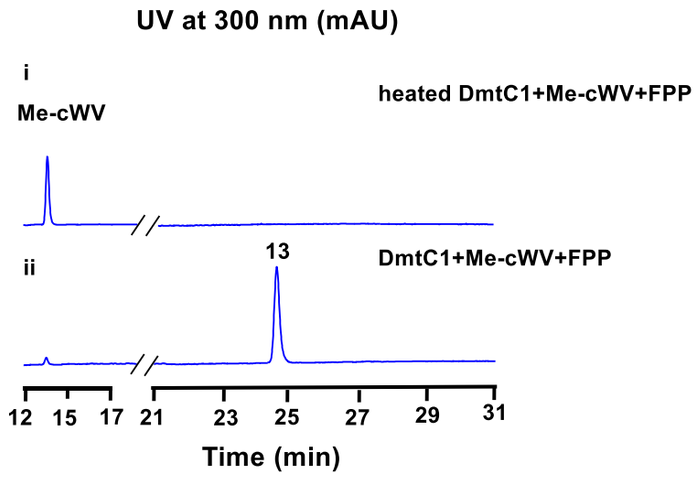

Figure S6. DmtC1-catalyzed reaction using Me-cWV and FPP as substrates, Related to Figure 4.

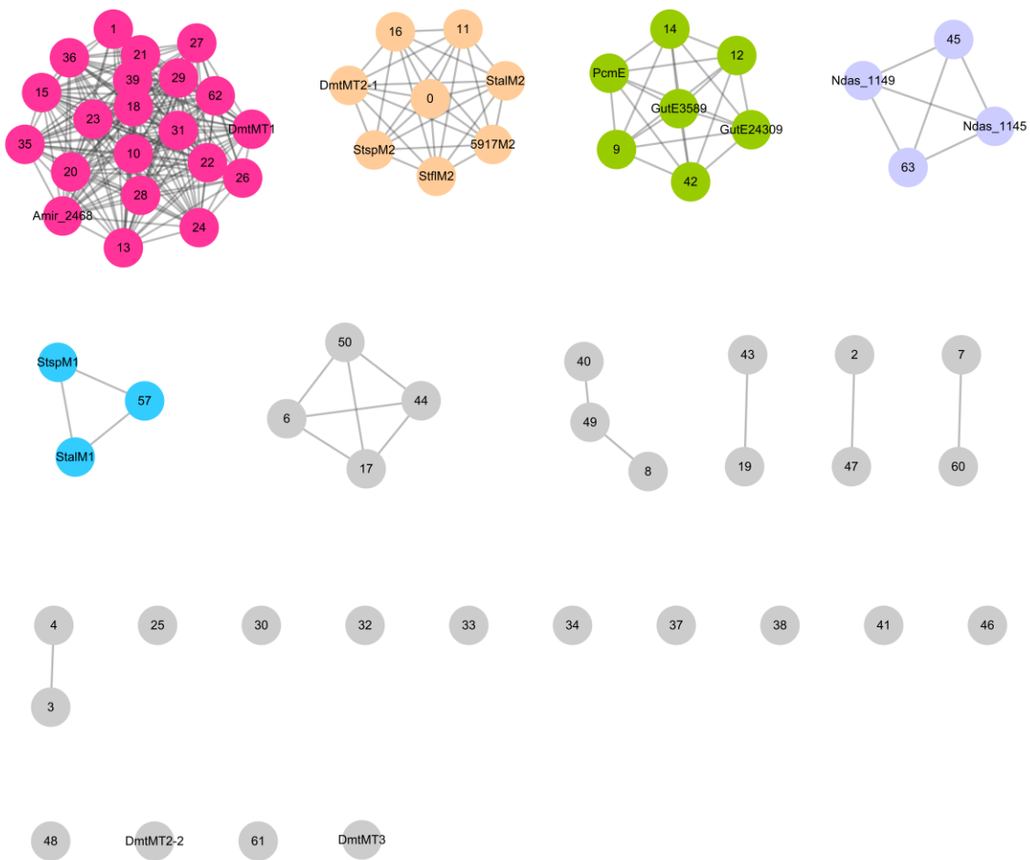

Figure S7. Sequence similarity networks (SSNs) of selected methyltransferases using an alignment score of 30. The details of the above proteins were shown in Data S3. Multiple MTs within this network are grouped with DmtMT1/Amir_4628 involved in the DKP-ring methylation. A couple of MTs clustered with known MTs are also included: four PcmE/GutE homologs (WP_078645497.1, WP_078897103.1, WP_078624486.1, and WP_023552492.1), two Ndas_1149/1145 homologs (WP_017534685.1 and WP_017534689.1), and one StspM1/StalM1 homolog (WP_027751607.1) , Related to Figure 1.

Table S1. Bacteria and plasmids used in this study, Related to Figures 2-6.

Strains or plasmids	Description	Reference or source
Strains		
E. coli Top10	Host strain of cosmid vector SuperCos1	Invitrogen
E. coli DH5*a*	Host strain for general cloning	Invitrogen
E. coli ET12567/pUZ8002	Host strain for conjugation	(Gust et al., 2003)
E. coli BW25113/pIJ790	Host strain for PCR-targeting	(Gust et al., 2003)
E. coli BL21-CodonPlus(DE3)	Protein expression host	Stratagene
E. coli BL21(DE3)	Protein expression host	Invitrogen
Streptomyces youssoufiensis OUC6819	Strain harboring the *dmt1* locus	(Che et al., 2012)
Streptomyces sp. NRRL F-5123	Strain harboring the *dmt2* locus	NRRL[a]
Streptomyces aidingensis CGMCC 4.5739	Strain harboring the *dmt3* locus	CGMCC[b]
ΔdmtMT1	*dmtMT1* inactivation mutant of *S. youssoufiensis* OUC6819	This study
Streptomyces coelicolor M1146	Host strain for heterologous expression	(Gomez‐Escribano and Bibb, 2011)
Plasmids		
SuperCosI	Amp^R, Kan^R, cosmid vector	Stratagene
pIJ773	Apr^R, source of *acc(3)IV-oriT* cassette	(Gust et al., 2003)
pIJ790	Cm^R, λ RED recombination plasmid	(Gust et al., 2003)
pSET152C	pSET152 derivative, with insertion of the *neo* gene from SuperCos1 at the sites of *Apa*I and *Sgr*AI	(Yao et al., 2018)
pIJ10500	Hyg^R, integrative plasmid containing the ϕBT1 integrase gene	(Kieser et al., 2000)
pET28a(+)	Kan^R, expression vector	Novagen
pET32a(+)	Amp^R, expression vector	Novagen
pWLI628	pET28a carrying *dmtMT1*	This study
pWLI629	pET28a carrying *dmtMT2-1*	This study
pWLI630	pET28a carrying *dmtMT3*	This study
pWLI631	pET32a carrying *dmtMT2-2*	This study
pWLI632	cosmid harboring *dmtMT1* gene from *S. youssoufiensis* OUC6819	This study
pWLI633	pWLI632 derivative where *dmtMT1* was replaced with *acc(3)IV-oriT* cassette	This study
pWLI634	pSET152C derivative harboring *dmtMT1* under the control of P_{gapdh}	This study
pWLI635	pSET152C derivative harboring *dmtMT2-1* under the control of P_{gapdh}	This study
pWLI636	pIJ10500 derivative harboring *dmtMT1* under the control of P_{hrdB}	This study
pWLI637	pIJ10500 derivative harboring *dmtMT2-1* under the control of P_{gapdh}	This study
pWLI638	pWLI636 derivative harboring *dmtMT2-1* under the control of P_{gapdh}	This study

a: Agricultural Research Service Culture Collection, NRRL

b: China General Microbiological Collection Center, CGMCC

Table S2. Primers used in this study, Related to Figures 2-6.

Name	Sequence (5'-3')
For DmtMT1, DmtMT2-1, DmtMT2-2 and DmtMT3 protein expression	
DmtMT2-1-FP	GGAATTCCATATGCAGCAGCAGACCACGGCG
DmtMT2-1-RP	CCGCTCGAGTCAGTTCCGCGCGGCGACG
DmtMT2-2-FP	CCGGAATTCATGGCCACTTCCTCGCCCTC
DmtMT2-2-RP	CCGCTCGAGCTAGCTCCGCGCCGCCCGC
DmtMT3-FP	GGAATTCCATATGACCTTCTCCCCCACCCC
DmtMT3-RP	CCGCTCGAGTCAGCGGGAGCGGCCGGTG
DmtMT1-FP	GGAATTCCATATGGGAAGTAAGCAGTACGAC
DmtMT1-RP	CCGCTCGAGCTTCACCGCCTCCAGGAC
For PCR-targeted mutagenesis of *dmtMT1*	
*dmtMT1*MF	GCGTAAGAGAGCGATTGCCGAGCGTGCGGGAAGGCGTGACattccggggatcc gtcgacc
*dmtMT1*MR	TGTCACTTCACCGCGCCACTTCACCGCCTCACTCGACCGCGtgtaggctggag ctgcttc
*dmtMT1*CF	CGTAAGAGAGCGATTGCCGA
*dmtMT1*CR	TCACCGCCTCACTCGACCG
*dmtMT1*EF	GTGGGAAGTAAGCAGTACGAC
*dmtMT1*ER	CTAGTCTAGATCACTTCACCGCCTCCAGGA
For heterologous expression of *dmtMT1* and *dmtMT2-1*	
dmtMT2-1-FP	ATGCAGCAGCAGACCACGG
dmtMT2-1-RP	CTAGTCTAGATCAGTTCCGCGCGGCGAC
dmtMT2-1-FP2	CCGCTCGAGCCGTCGCGGAAAGCTGGCC
dmtMT2-1-RP2	GGAATTCCATATGTCAGTTCCGCGCGGCGACG
dmtMT1-FP	GTGGGAAGTAAGCAGTACGAC
dmtMT1-RP	CCCAAGCTTTCACTTCACCGCCTCCAGG
pHFP	GGGGTACCTCTAGACCGCCTTCCGCCGG
pHRP	GAACAACCTCTCGGAACGTTG
pGFP	CCAATGCATCCGTCGCGGAAAGCTGGC
pGRP	GAACCGATCTCCTCGTTGGTG

Underlined red letters represent restriction sites. The primer pair of DmtMT1-FP/RP was also used for genomic library screening. The 3'-OH of pGRP and pHRP was phosphorylated. pHFP/pHRP and pGFP/RP were used for amplification of promotor P_{hrdB} and P_{gapdh}, respectively.

Table S3. Predicted functions of the four MT genes, Related to Figure 1.

Strain	Protein	Size (aa)	Proposed function	Homologs	
				Protein/Organism	Accession no. (Identity/Similarity %)
6819	DmtMT1	249	methyltransferase	Amir_4628/*Actinosynnema mirum* DSM 43827	ACU38461.1 (33.5/45.0)
F-5123	DmtMT2-1	294	methyltransferase	MitM/*Streptomyces lavendulae*	AAD28459.1 (36.7/49.8)
	DmtMT2-2	275	methyltransferase	UbiE/*Escherichia coli*	YP_026269.1 (16.4/25.3)
4.5739	DmtMT3	275	*N*5-glutamine methyltransferase	PrmC/*Chlamydia trachomatis*	AY600244.1 (24.2/34.6)

Transparent Methods

Strains

Streptomyces Strains

S. youssoufiensis OUC6819 strains were grown at 30 °C on R2YE agar medium. MS agar medium (3% soya flour, 2% mannitol, 2% agar powder) was used for the cultivation of *Streptomyces* sp. NRRL F-5123, *S. aidingensis* CGMCC 4.5739, and *S. coelicolor* M1146 strains. All the above *Streptomyces* strains were cultured in liquid TSBY medium (3% tryptic soya both, 10.3% sucrose, 0.1% tryptone, 0.05% yeast extract) at 30 °C for genomic DNA extraction. For the DMTs production, the strains were incubated in the production medium (1 % soluble starch, 2 % glucose, 4 % corn syrup, 1 % yeast extract, 0.3 % beef extract, 0.05 % $MgSO_4 \cdot 7H_2O$, 0.05 % KH_2PO_4, 0.2 % $CaCO_3$, and 3 % bay salt, pH = 7.0), followed by incubation at 30 °C, 220 rpm for 7 days.

E. coli Strains

E. coli strains including DH5α, BL21, BW25113/pIJ790 and ET12567/pUZ8002 were cultivated at 37 °C in Luria–Bertani (LB) liquid medium or on LB agar. When necessary, the medium was supplemented with 50 μg/mL of apramycin, 25 μg/mL of chloramphenicol, 100 μg/mL of kanamycin, 100 μg/mL of hygromycin, or 50 μg/mL of ampicillin.

DNA Manipulation and Plasmid Constructions

Plasmid extractions and DNA purification were carried out using commercial kits (OMEGA, BIO-TEK). Chromosomal DNA isolation, restriction endonuclease digestion, ligation, and transformation were performed according to standard procedures (Sambrook et al., 1989) or manufacturer's instructions.

For the expressions of *dmtMT1*, *dmtMT2-1*/*2* and *dmtMT3* in *E. coli*, the responding genes were amplified by polymerase chain reaction (PCR) using primer pairs listed in Table S2. *dmtMT1*, *dmtMT2-1*, and *dmtMT3* were digested with *Nde*I and *Xho*I, ligated into the pET28a(+) resulting in pWLI628-630; while *dmtMT2-2* was cloned into the *Eco*RI and *Xho*I sites of pET32a(+) resulting in pWLI631. After confirmation by sequencing, the resulting constructs pWLI628-630 were transformed into *E. coli* BL21 (DE3), and pWLI631 was transformed into *E. coli* BL21-CodonPlus (DE3).

For the combinatorial expressions of *dmtMT1* and *dmtMT2-1* in *Streptomyces* strains, the corresponding gene was put under the control of the constitutive promoter P_{gapdh} or P_{hrdB}. P_{gapdh} was amplified using primer pair of pGFP/3'-OH phosphorylated pGRP (Table S2) and digested with *Nsi*I; P_{hrdB} was amplified using primer pair of pHFP/3'-OH phosphorylated pHRP (Table S2) and digested with *Kpn*I. For expressions in OUC6819, *dmtMT1* and *dmtMT2-1* were respectively amplified with the primer pairs of *dmtMT1*EF/*dmtMT1*ER and *dmtMT2-1*-FP/*dmtMT2-1*-RP (Table S2) followed by digestion with *Xba*I; and then they were respectively ligated with P_{gapdh}, and cloned into the *Nsi*I and *Xba*I sites of pSET152C to give pWLI634-635. For expressions in M1146, *dmtMT1* was ligated with P_{hrdB} followed by insertion into the *Kpn*I and *Xba*I sites of pIJ10500 to give pWLI636; the P_{gapdh}-*dmtMT2-1* fragment was cloned into the *Nde*I and *Xho*I sites of pIJ10500 and pWLI636 to yield pWLI637-638. After confirmation by sequencing, the resulting plasmids pWLI636-638 were passed through *E. coli* ET12567/pUZ8002, and then introduced into *S. coelicolor* M1146/*dmtB1C1* or *S. coelicolor* M1146/*dmtA1B1C1 via* conjugation (Kieser et al., 2000).

Protein Expression and Purification

The expressions of *dmtMT1*, *dmtMT2-1*, *dmtMT2-2* and *dmtMT3* followed the same protocol and were detailed as follows. Overnight culture of *E. coli* harboring the expression plasmid (10 mL) was inoculated into 1 L of LB medium (containing 50 μg/mL of kanamycin, or 25 μg/mL of chloramphenicol and 50 μg/mL of ampicillin) and grown at 37 °C, 220 rpm. Expression was induced at an OD_{600} of approximately 0.6 by addition of isopropyl β-D-thiogalactopyranoside (IPTG) (with final concentration of 0.05 mM), and cultivation was continued for additional 16 hrs at 16 °C**.**

The cells were pelleted by centrifugation (15 min at 8,000 x *g*) and resuspended in 30 mL of binding buffer A (0.05 M Tris-HCl, 0.5 M NaCl, 5.0% glycerol (v/v), pH 7.5, containing cOmplete^{TM} protease inhibitor cocktail). The resuspended cells were lysed by sonication in an ice-water bath with an ultrasonic processors VCX750 (Sonics & Materials Inc, PA, USA), and were centrifuged at 10,000 x *g* for 30 min at 4 °C. The resulting supernatant was applied to a HisTrap HP column (1 mL, GE Healthcare) and the His-tagged protein was eluted with a linear gradient of imidazole (30–500 mM) in the binding buffer using an ÄKTA Purifier system. After SDS–PAGE analysis, fractions containing pure protein were pooled, concentrated and exchanged to Tris buffer (0.025 M Tris-HCl, 0.02 M NaCl, and 10.0% glycerol, pH 7.5) by using Amicon Ultra-15 30-kDa cutoff centrifugal concentrator (Millipore).

***In Vitro* Assays**

For *in vitro* experiments, each of the recombinant DmtMT1, DmtMT2-1/2, and DmtMT3 (10 μM) was incubated with 0.5 mM DKPs/pre-DMTs/DMTs (Sun et al., 2013) and 0.5 mM SAM in Tris buffer [50 mM Tris (pH 8.0) and 0.1 mM DTT] at 30 °C for 12 hrs. Reactions were stopped by the addition of equal volume of methanol and mixed by vortexing. For the detection of pre-DMTs/DMTs, the mixtures were subjected to HPLC analysis, using a YMC-Pack ODS-AQ C18 column (150 mm × 4.6 mm, particle size of 5 μm, pore size of 120 Å) under the program: phase A consisting of 0.1% (v/v) formic acid and ddH_2O, phase B consisting of 0.1% (v/v) formic acid and acetonitrile; 50% B (0–5 min), 50% to 100% B (5–30 min), 100% B (30–45 min), at a flow rate of 1 mL min^{-1} and UV detection at 300 nm. For the detection of DKPs, the program was set as follows: 10% B (0–5 min), 10% to 50% B (5–25 min), 100% B (25–35 min), at a flow rate of 1 mL min^{-1} and UV detection at 280 nm. For probing substrate promiscuity of DmtMT1, different DKPs (0.5 mM) were tested as described above and were analyzed with HPLC-MS^2; the enzymatic reactions were performed in triplicate, and all rates were calculated with their peak areas at 280 nm.

The assay of DmtMT1 with cWV was scaled up and subsequently subjected to a semi-preparative HPLC column (YMC-Pack ODS-AA C18 column, 120 Å, 250×10 mm, 5 μm) for purification. The resulting Me-cWV was stored at -20 °C until use. The enzymatic assay of DmtC1 was carried out in 50 mM Tris-HCl buffer (pH 8.0) with 2.5 mM $MgCl_2$, containing 10 μM DmtC1, 1 mM Me-cWV, and 0.2 mM FPP at 30 °C. After 1 hr, the reaction was quenched by the addition of equal volume of methanol and mixed by vortexing. The mixture was centrifuged at 17,000 x *g* for 20 min to remove proteins. The supernatant was then applied to YMC-Pack ODS-AQ C18 column with UV detection at 300 nm under the program: 10% B (0–5 min), 10% to 50% B (5–15 min), 80% to 100% B (15–25 min), at a flow rate of 1 mL min^{-1} (phase A, 0.1% formic acid in ddH_2O; phase B, 100% acetonitrile supplemented with 0.1% formic acid).

Gene Inactivation, Complementation, and Overexpression in *S. youssoufiensis* OUC6819

Inactivation of *dmtMT1* in *S. youssoufiensis* OUC6819 was performed using the REDIRECT Technology according to the literature protocol (Yao et al., 2018). The genomic library was screened using the primer pair of DmtMT1-FP/ DmtMT1-RP, giving positive cosmid pWLI632. The *aac(3)IV-oriT* resistance cassette was amplified with primer *dmtMT1*MF/ *dmtMT1*MR (Table S2) using pIJ773 (Gust et al., 2003) as template and was transformed into *E. coli* BW25113/pIJ790 containing pWLI632 to replace an internal region of *dmtMT1*, resulting in

mutant cosmid pWLI633. pWLI633 was passed through *E. coli* ET12567/pUZ8002 and was then introduced into *S. youssoufiensis* OUC6819 by intergenic conjugation using mycelia as recipients. The mutant *ΔdmtMT1* was selected by the apramycin-resistant and kanamycin-sensitive phenotype and was further confirmed by PCR using the primer pair of *dmtMT1*CF/*dmtMT1*CR (Table S2). For overexpression, pWLI634-635, containing intact *dmtMT1* and *dmtMT2-1*, were respectively passed through *E. coli* ET12567/pUZ8002 and introduced into the wild-type *S. youssoufiensis* OUC6819 *via* conjugation. pWLI634 was further introduced into *ΔdmtMT1* for genetic complementation.

Production and Analyses of DMTs

Spores of *Streptomyces* strains were incubated into 50 mL of production medium in 250 mL Erlenmeyer flasks fitted with glass beads, at 30 °C and 220 rpm for 7 days. The supernatants were extracted twice with an equal volume of ethyl acetate, and the combined ethyl acetate extracts were concentrated *in vacuo* to afford residue A. The precipitated mycelia were extracted twice with acetone. The extracts were combined, and acetone was evaporated *in vacuo* to yield residue B. The combined residues were dissolved in methanol and filtered through a 0.2 μm filter. The resulting fermentation products derived from *ΔdmtMT1*, genetic complementation and overexpression strains were subjected to HPLC analysis, eluting with a linear gradient of B/A in 40 min (phase A, 0.1% formic acid in ddH_2O; phase B, 100% acetonitrile supplemented with 0.1% formic acid; flow rate: 1 mL min^{-1}; wavelength: 300 nm) using a YMC-Pack ODS-AQ C18 column. The fermentation products of heterologous expression strains were detected under the identical conditions used for analyzing the DmtMT2-1-cataylzed reactions using pre-DMTs/ DMTs as substrates.

Isolation and Characterization of the Methylated pre-DMTs and DMTs

For isolation of DmtMT2-1 enzymatic products, the *in vitro* assays contained pre-DMTs/DMTs (0.5 mM) and DmtMT2-1 (30 μM) were scaled up to 30 mL. The reactions were extracted three times with an equal volume of ethyl acetate and concentrated *in vacuo*. The extracts were further purified by eluting with linear gradient from 80 to 100% B/A (phase A: ddH_2O; phase B: acetonitrile, 1.5 mL min^{-1}, UV detection at 300 nm) in 40 min using a semi-preparative HPLC column (YMC-Pack ODS-AA C18 column, 120 Å, 250×10 mm, 5 μm). For isolation of pre-DMT F (**13**), the reaction consisted of cWV (0.5 mM), SAM (1 mM), FPP (0.5 mM), DmtMT1 (50 μM), DmtC1 (30 μM), and $MgCl_2$ (2.5 mM) in Tris-HCl buffer (50 mM, pH 8.0) was performed, the mixture was treated in the same way as that of the DmtMT2-1-catalyzed reactions.

To isolate compound **16**, The *S. youssoufiensis* OUC6819 expressing *dmtMT2-1* was fermented in a total volume of 15 L. The fermentation cultures were treated as described above. The residues were applied to reversed-phase C18 open column, eluting with a gradient eluent of 20%–100% methanol to give five fractions (Fr.1~Fr.5) for each fermentation culture. Compound **16** was obtained by further separation of the Fr.4, eluting with the identical program used for isolation of DmtMT2-1 enzymatic products. The structures of the above compounds were characterized by HR-ESI-MS carried out on Thermo LTQ Orbitrap XL mass spectrometer, and NMR spectroscopy recorded with Bruker Avance III 600 spectrometers. All spectra were processed with MestReNova.6.1.0 (Metrelab), and chemical shifts were referenced to those of the solvent DMSO-d_6 signals.

Bioinformatic Analysis

ORF assignments and their proposed functions were accomplished by using FramePlot4.0 beta (Ishikawa and Hotta, 1999) (http://nocardia.nih.go.jp/fp4). Sequence comparisons and database searches were accomplished with BLAST programs (McGinnis and Madden, 2004) (http://blast.ncbi.nlm.nih.gov/Blast.cgi). 71 CDPS-associated MTs listed in Data S3 were extracted from the NCBI database (https://www.ncbi.nlm.nih.gov/protein); and Enzyme Function

Initiative-Enzyme Similarity Tool (EFI-EST) (Gerlt et al., 2015) was used to construct the sequence similarity network using an alignment score of 30. The network was visualized in Cytoscape (Shannon et al., 2003).

Supplemental References

Che, Q., Zhu, T., Qi, X., Mandi, A., Kurtan, T., Mo, X., Li, J., Gu, Q., and Li, D. (2012). Hybrid isoprenoids from a reeds rhizosphere soil derived actinomycete *Streptomyces* sp. CHQ-64. Org. Lett. *14*, 3438-3441.

Gerlt, J.A., Bouvier, J.T., Davidson, D.B., Imker, H.J., Sadkhin, B., Slater, D.R., and Whalen, K.L. (2015). Enzyme Function Initiative-Enzyme Similarity Tool (EFI-EST): A web tool for generating protein sequence similarity networks. Biochim Biophys Acta *1854*, 1019-1037.

Gomez‐Escribano, J.P., and Bibb, M.J. (2011). Engineering *Streptomyces coelicolor* for heterologous expression of secondary metabolite gene clusters. Microb. Biotechnol. *4*, 207-215.

Gust, B., Challis, G.L., Fowler, K., Kieser, T., and Chater, K.F. (2003). PCR-targeted *Streptomyces* gene replacement identifies a protein domain needed for biosynthesis of the sesquiterpene soil odor geosmin. Proc Natl Acad Sci U S A *100*, 1541-1546.

Ishikawa, J., and Hotta, K. (1999). FramePlot: a new implementation of the frame analysis for predicting protein-coding regions in bacterial DNA with a high G + C content. FEMS Microbiol. Lett. *174*, 251-253.

Kieser, T., Bibb, M.J., Buttner, M.J., Chater, K.F., and Hopwood, D.A. (2000). Practical *Streptomyces* genetics, Vol 291 (John Innes Foundation Norwich).

McGinnis, S., and Madden, T.L. (2004). BLAST: at the core of a powerful and diverse set of sequence analysis tools. Nucleic Acids Res. *32*, W20-W25.

Sambrook, J., Fritsch, E.F., and Maniatis, T. (1989). Molecular cloning: a laboratory manual (Cold spring harbor laboratory press).

Shannon, P., Markiel, A., Ozier, O., Baliga, N.S., Wang, J.T., Ramage, D., Amin, N., Schwikowski, B., and Ideker, T. (2003). Cytoscape: a software environment for integrated models of biomolecular interaction networks. Genome Res. *13*, 2498-2504.

Sun, Y., Li, R., Zhang, W., and Li, A. (2013). Total synthesis of indotertine A and drimentines A, F, and G. Angew. Chem. *52*, 9201-9204.

Yao, T., Liu, J., Liu, Z., Li, T., Li, H., Che, Q., Zhu, T., Li, D., Gu, Q., and Li, W. (2018). Genome mining of cyclodipeptide synthases unravels unusual tRNA-dependent diketopiperazine-terpene biosynthetic machinery. Nat. Commun. *9*, 4091.